Chapter 5
Data-driven modeling of the BARC component using Dynamic Mode Decomposition

Celso T. do Cabo, Raymond Joshua, and Zhu Mao*

Abstract The vibrational behavior of structures is of great importance in a variety of applications. Typically, laboratory tests are designed to obtain such information from the system. However, in many cases, those applications have complex behavior or are too large, making it unfeasible to obtain the characteristics of the whole structure, leading to tests only in critical components. In such cases, modeling the boundary conditions of a specific component while predicting how it will behave in the real world can be challenging. The box assembly with a removable component (BARC) was a challenge developed to study the effects of the boundary conditions in a component when performing a laboratory test versus the full structure behavior in operation. The approaches predicting behaviors of a component in the real world often rely on physical information about the system, for example, using FEA models or coupling the frequency response of the system. With the increased interest in data-driven and machine learning approaches, dimension reduction models are widely used to reduce the order of a system while maintaining important information. Dynamic mode decomposition (DMD) uses the Koopman operator to learn the dynamic modes of the system and then predict its future state. This work proposes the use of the Koopman operator and DMD to predict the behavior of the component of BARC based on data-driven knowledge.

Keywords Model order reduction · Structural dynamics · Dynamic mode decomposition · BARC

Introduction

The dynamical behavior of structures is of critical importance for a variety of applications. To obtain the system's behavior, often laboratory tests are conducted, or simulation models are created. However, in many cases, those structures will have multiple components and can be too large to perform a laboratory test under the same conditions as the real world. One solution for such cases is to perform tests in critical components of the structure, trying to predict the behavior of the interaction between the critical component and the rest of the system [1, 2]. Multiple different techniques were developed over the years to perform substructuring based on the dynamical behavior of a complex system. Mainly, using modal analysis techniques, employing reduction techniques, and modifying the boundary conditions for the components, or assuming the behavior of the interfaces [3, 4]. Such techniques can also be employed with the aid of FEA models for linear and nonlinear cases [5]. Among the substructure models, the boundary assembly with removable component (BARC) was developed as a boundary condition challenge to study the effect of the interaction of a certain component in a large structure [6]. Since its creation, several studies have been performed on this challenge, ranging from works on the effect of types of excitation to substructure techniques [7, 8], testing conditions when dealing with connections between components [9] or different algorithms that can predict the behavior of the structure [10, 11].

Celso T. do Cabo · Zhu Mao
Department of Mechanical and Materials EngineeringWorcester Polytechnic Institute, Worcester, MA 01609
e-mail: ctdocabo@wpi.edu; zmao2@wpi.edu

Raymond Joshua
Honeywell Federal Manufacturing & Technologies, LLC operates the Kansas City, National Security Campus for
the United States Department of Energy / National NuclearSecurity Administration under Contract Number DE-NA0002839
e-mail: rjoshua@kcnsc.doe.gov

*NSC-614-5856
DE-NA0002893

Kristin B. Zimmerman, PhD (eds.), *Dynamic Substructuring & Transfer Path Analysis, 2026, Vol. 4*, Conference Proceedings
of the Society for Experimental Mechanics Series, https://doi.org/10.1007/978-8-743-81443-6_5

Recently, with the increased interest in data-driven approaches, multiple techniques are employed in the field of structural dynamics since often the behavior of the structure is difficult to predict analytically or requires prior physical knowledge of the component studied. Among them, order reduction techniques are often employed to reduce the complexity of the system and increase its interpretability. Some of those techniques are well known in different applications, such as Principal Component Analysis (PCA), or Proper Orthogonal Decomposition (POD), which were previously employed to decompose signals using Singular Value Decomposition (SVD) for fluid dynamics or vibration [12–14]. One of the newer techniques for data-driven order reduction is the Dynamic Mode Decomposition (DMD), which was initially developed by Schmid [15], and later implemented in multiple applications, including fluid dynamics and vibration cases using video-based sensing [16–18]. This technique predicts the future timesteps of a system by approximating the Koopman operator in a matrix format, and the obtained matrix will be a square matrix that can be decomposed into a spatial and temporal domain to obtain the mode shapes and modal responses of the structure [19]. Since the matrix obtained depends on the sensors used for the experiment, this work proposes using DMD and other techniques, such as PCA, to model the system's behavior from the component measurements and the mode shapes obtained using solely a data-driven approach. For that, a simulation of an impact test was performed in the BARC for both the full structure and the component alone. The mode shapes and modal responses were then compared to verify the accuracy of the data-driven approach in decomposing complex behavior systems.

Data-driven Dimension Reduction

Among the well-known data-driven techniques for dimension reduction, techniques such as singular value decomposition (SVD) and principal component analysis (PCA) are famous in the machine learning domain to reduce the order of the dataset used in a certain problem. When working with physical problems, such as fluid flow or vibration in continuous structures, proper orthogonal decomposition (POD) is also well-known and widely employed in order reduction problems. Both techniques work by performing an SVD of the original dataset or by performing an eigen decomposition in the covariance matrix of the data. The SVD decomposes the original measurement $[X]$ into three different matrices as shown in Equation (1).

$$[X] = [U]\,[\Sigma]\,[V]^T \tag{1}$$

The matrix $[U]$ is the matrix of unitary vectors representing the spatial components of $[X]$, while $[V]$ is the matrix unitary vector with the temporal components and $[\Sigma]$ is the diagonal matrix with the variation of each of the components. Dynamic Mode Decomposition (DMD) also uses an eigen decomposition to obtain the mode shapes and natural frequencies of the data. However, it uses the Koopman operator to obtain a time-invariant matrix $[A]$ and performs the eigen decomposition in this matrix. This matrix is computed such that it can predict the next step based on the current one, as presented in Equation (2).

$$[X'] \approx [A]\,[X] \tag{2}$$

Where, $[X']$ is the future state matrix, going from time step 2 to n and $[X]$ the current state matrix from the time step 1 to $n-1$ and $[A]$ is the Koopman operator matrix. To calculate $[A]$, a SVD can be performed on the matrix $[X]$ and rearranged. In addition, a low-rank representation $\left[\tilde{A}\right]$ can also be performed to reduce the computational cost for high-dimensional problems (e.g., video-based sensing). The calculation is presented in Equation (3).

$$\left[\tilde{A}\right] \approx [U]^T\,[A]\,[U] = [U]^T\,[X']\,[V]\,[\Sigma]^{-1} \tag{3}$$

The matrices $[U]$, $[\Sigma]$ and $[V]$ are the same matrices obtained by the SVD of $[X]$ explained from Equation (1). After calculating the low-rank approximation of the Koopman operator, a new eigen decomposition is performed as shown in Equation (4).

$$\left[\tilde{A}\right]\left[\tilde{W}\right] = \left[\tilde{W}\right][\Lambda] \tag{4}$$

Here, $\left[\tilde{W}\right]$ is the matrix of eigenvectors of the low-rank representation of the Koopman operator, and $[\Lambda]$ is the diagonal matrix with the eigenvalues of the system. Finally, the DMD modes can be computed as shown in Equation (5).

$$[\Phi] = [X']\,[V]\,[\Sigma]^{-1}\left[\tilde{W}\right] \tag{5}$$

Unlike other traditional techniques, such as PCA, DMD will compute the time response for each DMD mode based on an exponential approximation, which is described by Equation (6).

$$t_{DMD} = be^{\omega t} \tag{6}$$

b is a scale factor, computed from the initial condition of the system and ω is one of the natural frequencies of the system. These natural frequencies are estimated based on the eigenvalues obtained in Equation (4) as presented in Equation (7).

$$\omega_k = \frac{\log\lambda_k}{dt} \tag{7}$$

λ_k is the k^{st} term of the eigenvalue matrix $[\Lambda]$ and dt is the size of the timestep collected in the measurement. Finally, the approximation of the total response can be calculated from Equation (8).

$$\left[\hat{X}\right] \approx [\Phi] \times [t_{DMD}] \tag{8}$$

In addition to the traditional approach to calculate the mode shapes and time response, another model was developed for DMD, which uses an optimization approach. The algorithm is called optimized DMD or opt-DMD, and it tries to minimize Equation (9) below [20].

$$\min \|[X] - [\Phi] \times [t_{DMD}]\| \tag{9}$$

BARC simulations

To extract the dynamic behavior of the BARC and its components, two FE simulations were performed using Abaqus. The initial design was provided by the Sandia National Laboratory. The simulations consisted of a modal analysis of the structure to obtain the eigenvalues and vectors of the structure. Afterwards, a new dynamic simulation of an impact test was conducted, by giving the structure an impact in the top part of the component with the base of the BARC in a fixed boundary condition. The data was collected in 9 nodes located between the top part of the component, the nodes in the connection between the component and the remaining of the structure, and two locations on the sides of the structure. The measurement nodes are highlighted in red in Figure 1. In addition, the displacement in X, Y, and Z directions is collected, as well as the rotation in all directions, leading to six DOFs for each node. The dynamic simulation had a sampling frequency (f_s) of 10kHz and 500 timesteps were collected.

Results and Discussion

Aiming to compare how different data-driven techniques can describe the system's behavior, both PCA and DMD were employed in the BARC simulation. As described in the previous section, the data was collected for both the full structure simulation, presented in Figure 1, and the simulation of the component only. In addition, initially, only points in the component were extracted to allow a comparison with the same number of DOFs. Starting with five points located in the BARC component, leading to a 30-DOF measurement. When performing PCA in the system, the comparison of the mode shapes for full and substructure, as well as the variation for each of the components, is presented in Figure 2.

Figure 2(a) presents the variation of each component for both the full and substructure. Notice that most of the variation of the data occurs within the first four components, and after that, the values converge to zero. This leads to a very small amplitude of motion for those modes, or they are composed only of the noise of the measurements. In Figure 2(b) the comparison between the PCA modes or components is shown for both the full structure and substructure. Since the variation of the data occurs only in the first four modes, it can be noticed that the MAC between them is close to 100% and is on the diagonal of the matrix. Therefore, it is possible to compare the mode shapes and time signal for the same coefficients.

Figure 3(a) presents the time reconstruction for each of the modes (V matrix for SVD). It can be seen that the first two components have a similar behavior in both the full and substructure, with a slight change in the natural frequency for the second component. This happens since the change in boundary conditions in the component will lead to different natural frequencies of the system. However, the mode shapes are equivalent to both simulations. However, in the third and fourth components, the behavior of the substructure already behaves similarly to random noise, which can also be seen in the frequency plots. Based on Figure 2(a) the variation of the substructure declines significantly after the second component. Meanwhile, the variation for the full structure is higher until the fifth component. Since the natural frequencies of the component are higher than the full structure, the dynamic simulation was able to capture only the first two mode shapes. In addition, PCA is not capable of completely isolating the natural frequencies of each component. For high-frequency modes, it can be seen that one component has multiple natural frequencies. Moreover, PCA orders the components based on the variation of the data. Therefore, it is required to calculate the Fourier transform of the data to obtain the natural frequency of the system.

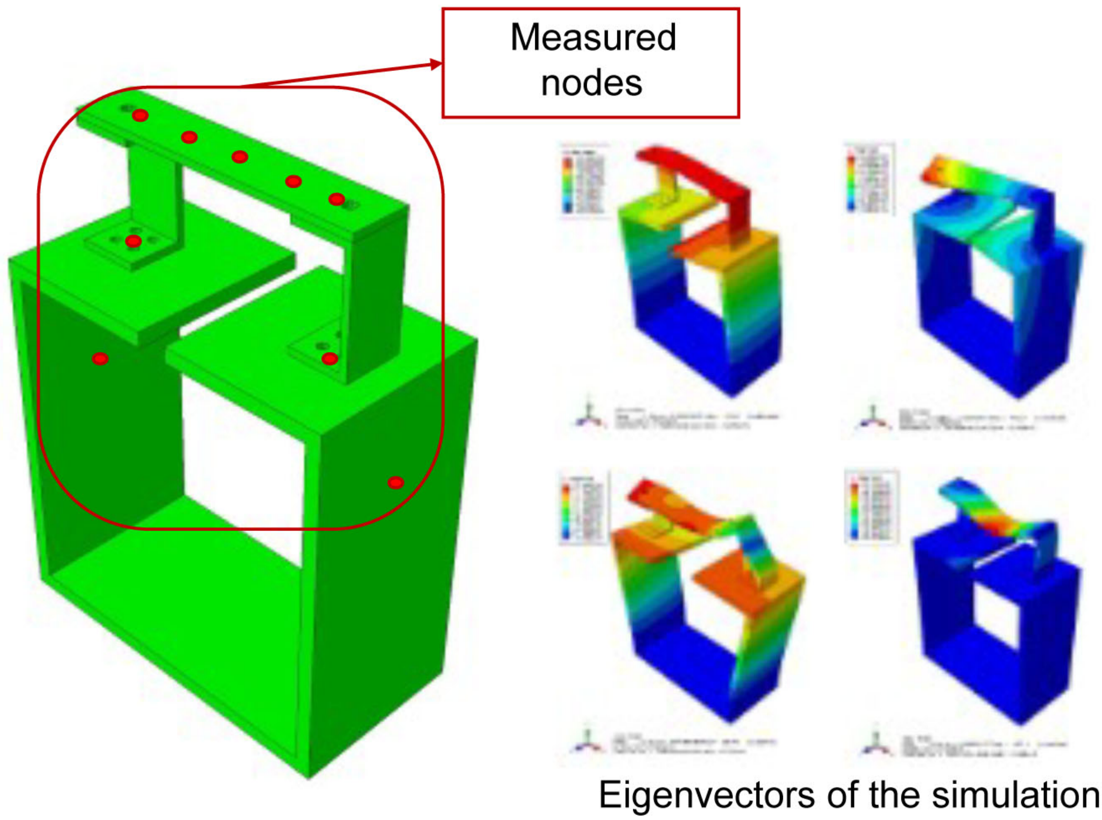

Fig. 1 BARC simulation, measured nodes in the left, examples of mode shapes with the fixed boundary condition in the right

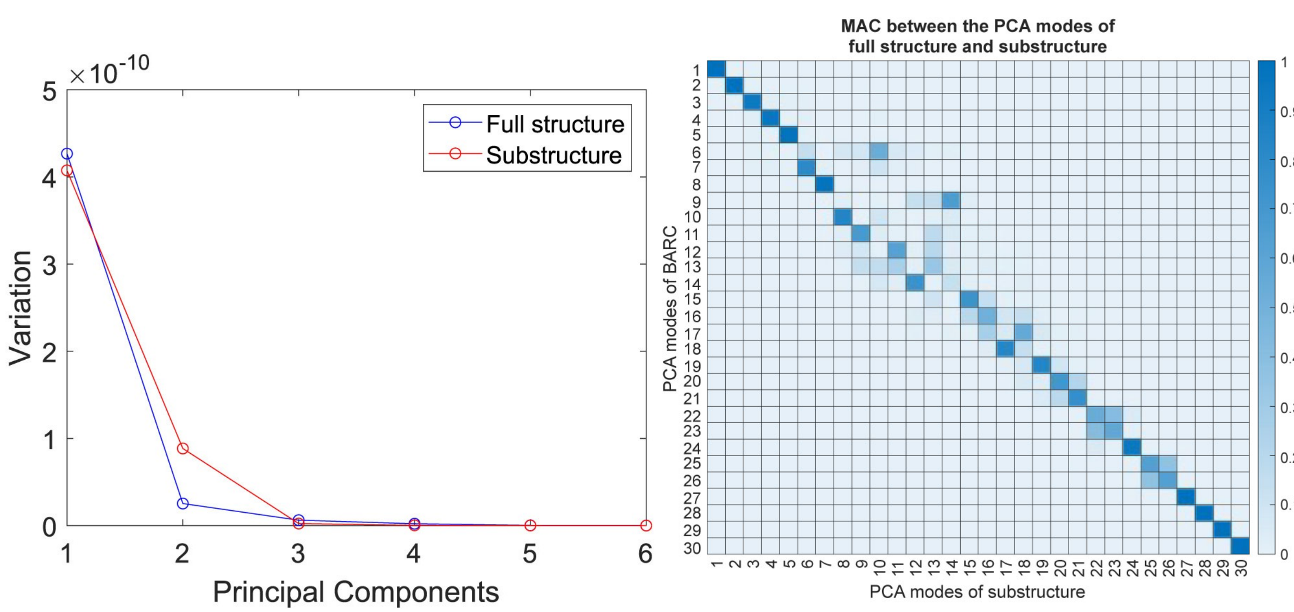

(a) (b)

Fig. 2 PCA applied to the BARC simulation; (a) presents the variation of each component and (b) the MAC between the components obtained from the full structure and substructure

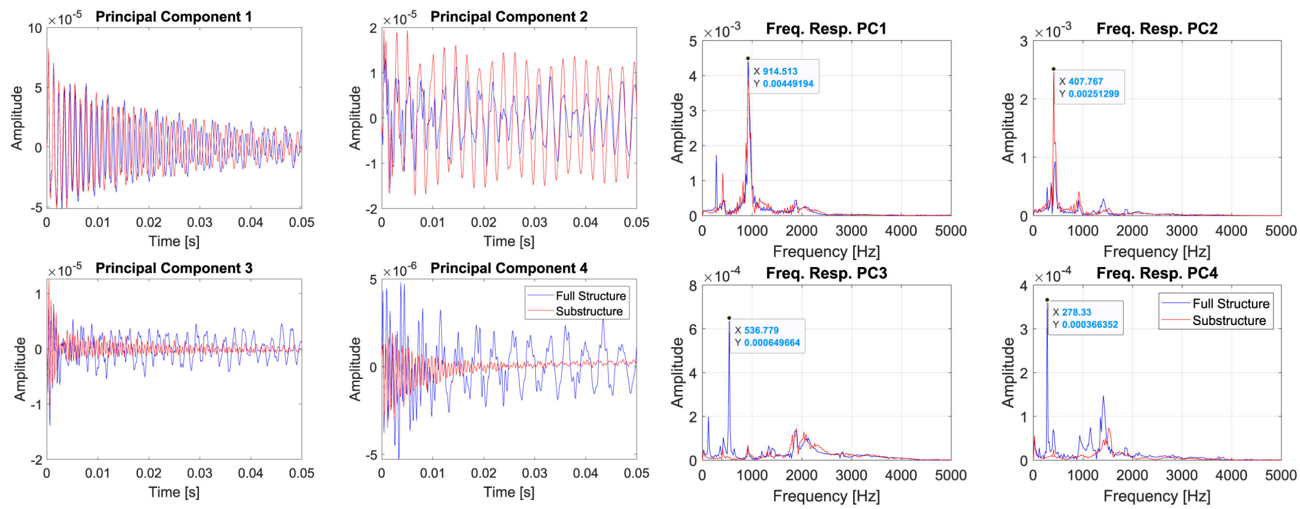

(a) (b)

Fig. 3 PCA reconstruction of each component in (a) time domain and (b) frequency domain

After employing PCA, the optimized DMD was performed in the same simulation. Since DMD estimates each time response by using an exponential function, which for vibrational systems will lead to complex eigenvalues. This will lead to pairs of eigenvalues that will be compared for both full and substructure. Figure 4(a) shows the eigenvalues of the optimized DMD applied to the substructure and full structure in red and blue, respectively. In addition, DMD is capable of estimating the natural frequency based on the eigenvalue, so the Y-axis values shown are the natural frequencies of the system. However, due to how the algorithm sorts the eigenvalues, those natural frequencies do not match every application. The highlighted frequencies shown in the plot have a similar natural frequency, and the dashed lines in red show frequencies that are different, but the modes obtained have a similar behavior. This behavior often happens with transition behavior in the measurement. In Figure 4(b) presents the MAC between the modes, with the same modes highlighted.

Figure 5(a) shows the time estimation for some of the eigenvalues. Subplot 1 (top left) shows the time reconstruction for the 2,000Hz eigenvalue, while Subplots 2 and 4 show the reconstruction for the 1,000Hz eigenvalue. The third subplot has

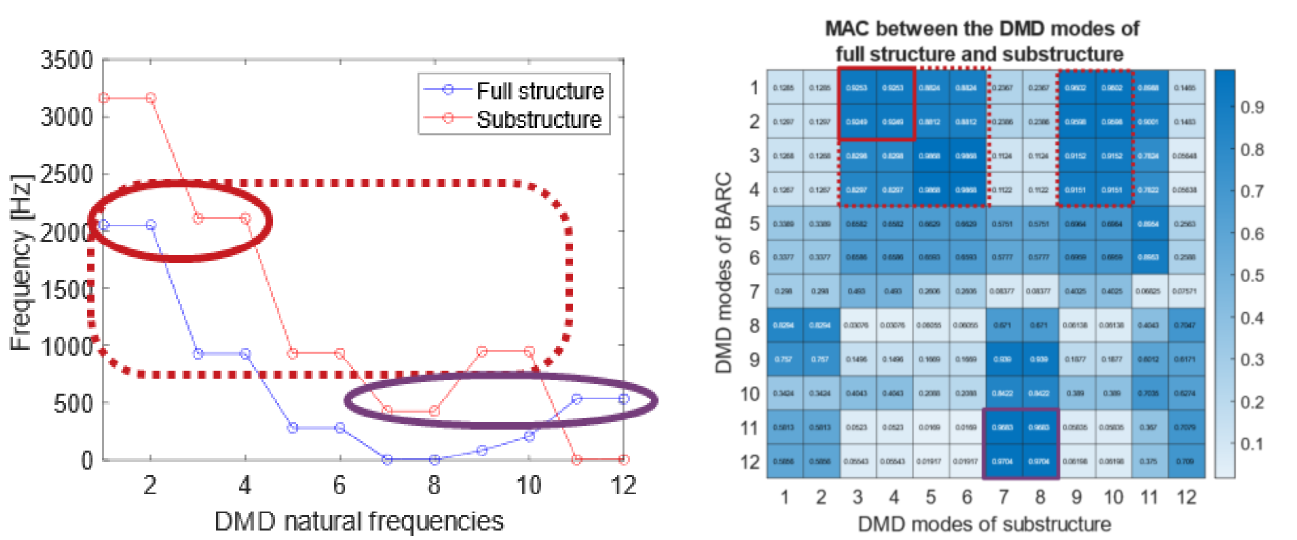

(a) (b)

Fig. 4 Optimized DMD applied to BARC; (a) Eigenvalues and their corresponding natural frequencies, and (b) MAC between the modes of the full structure and substructure

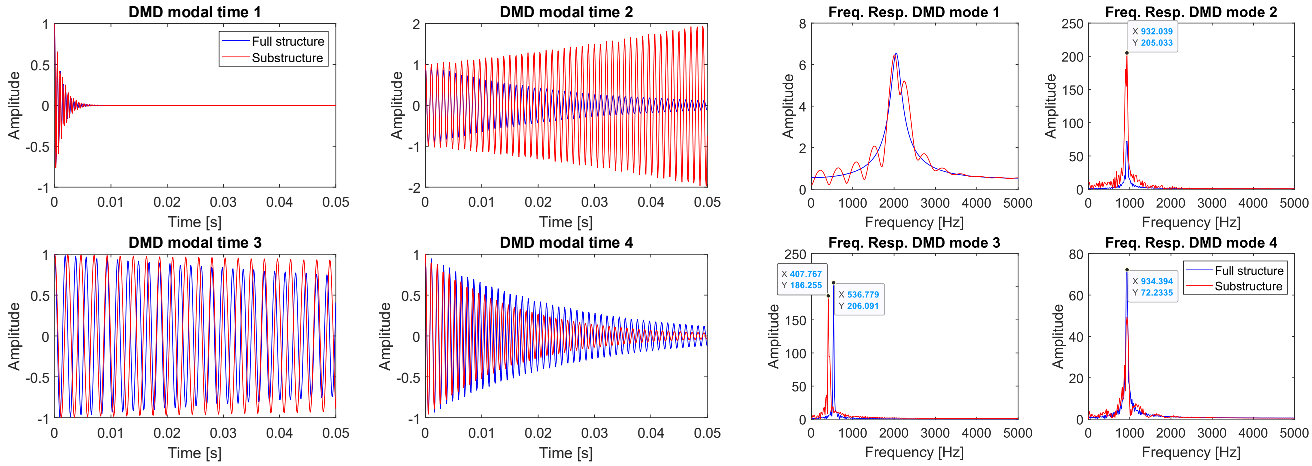

(a) (b)

Fig. 5 DMD reconstruction for four eigenvalues, (a) time domain reconstruction and (b) frequency response of the reconstruction

the lower frequency mode (around 500Hz). Different from PCA, DMD estimates each mode using an exponential function, which will possess only one pure tone. This can be observed in Figure 5(b) on the Fourier transform of (a). The frequency aligns well for both models, except for the third subplot, which has a small change in frequency between the models.

In addition, since the DMD estimates the modal response based on an exponential approximation, the frequency response for each mode shape will have a single frequency isolated, while PCA has multiple frequency components. However, PCA approximates the mode shapes based on the variation of data. Therefore, if the modes have a similar behavior, they will be in order as presented in Figure 2(b), while DMD has a different sorting that will not exactly match for different tests.

When employing the exact DMD (original approach as described from Equation (2) to (8)), if the dataset obtained has a small dimension or, in other words, smaller measuring points versus timesteps recorded, the mode shape estimation will have a good accuracy. However, the time estimation will be wrong. Aiming to reduce the time reconstruction error to the BARC, preliminary results of using the Koopman operator to predict the time response of the model were obtained. For that, the full rank matrix $[A]$ was computed for the simulation, and it is shown in Figure 6(a). In this case, some of the DOFs extracted in

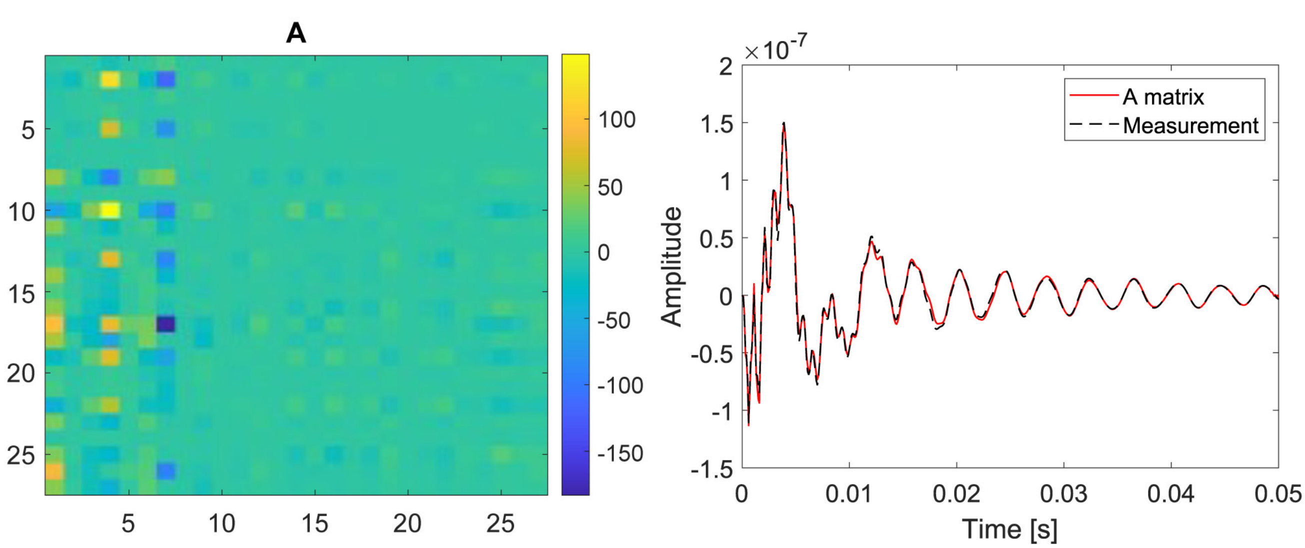

(a) (b)

Fig. 6 Full-rank A matrix employed to the BARC; (a) shows the full-rank Koopman operator and (b) the time reconstruction for one of the simulation nodes the experiment had a very low amplitude compared to others, therefore, the values close to zero were disregarded, leading to a 27 DOF system When performing the signal reconstruction following Equation (2), it can be seen in (b) that the signal has a very similar response to the simulation.

In Figure 7, a comparison of all the DOF extracted from the simulation and the reconstruction signal is presented. The TRAC for the diagonal values is close to 100%, which means that the signal reconstruction is effective with the Koopman operator, but the TRAC value is also high at several other locations. This can be caused by similar measurements, since the simulation possesses simple excitation, which might excite only a limited number of modes. In addition, due to the complexity of the structure, the modes can have similar behavior in specific locations, increasing the difficulty of obtaining perfectly orthogonal measurements.

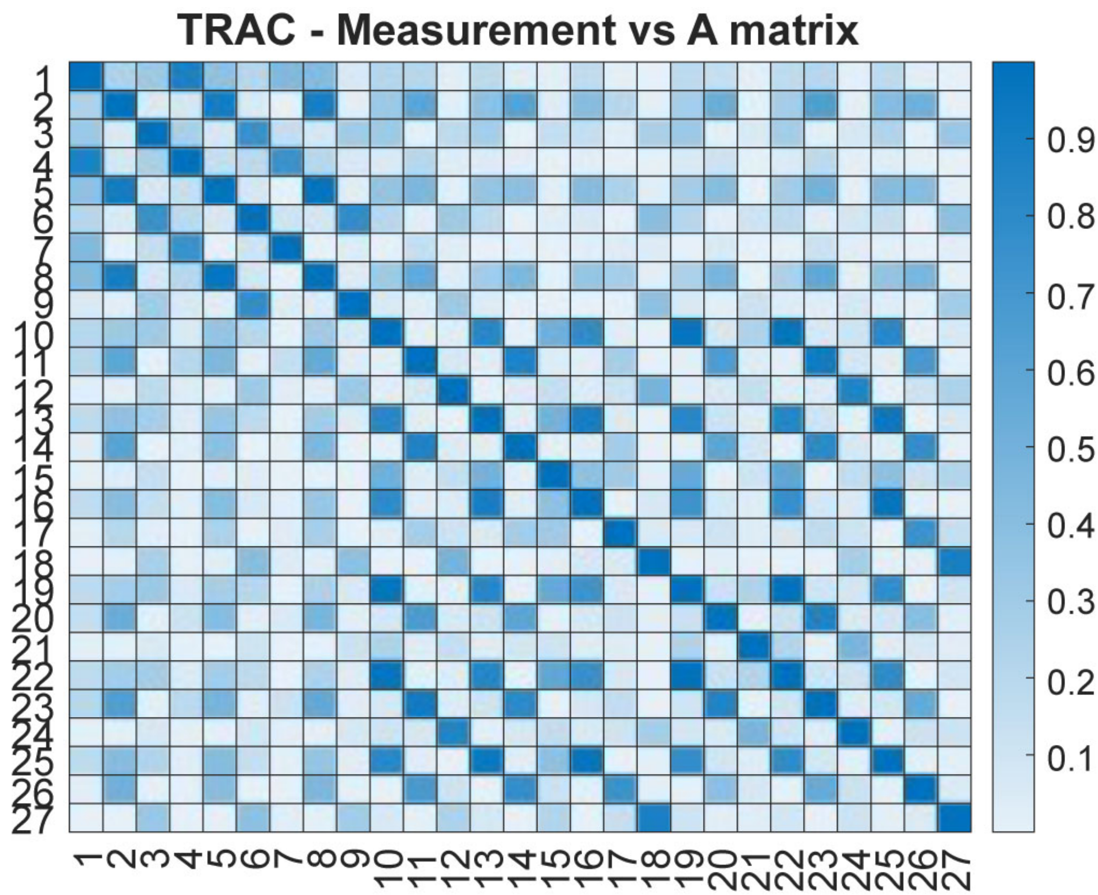

Fig. 7 TRAC between the BARC simulation and the signal reconstruction performed by the A matrix, for 27 DOFs

Conclusion

This work presented an analysis of data-driven techniques employed to substructure problems, more specifically, to the BARC challenge. Usually, such problems are challenging and require previous knowledge of the structure. Being able to obtain some information, such as mode shapes and natural frequencies, as well as correlating such information using only what was acquired in an experiment, can facilitate further analysis on complex structures. PCA and other traditional techniques are capable of obtaining the mode shapes of the system in an accurate manner. But the technique has limitations on frequency isolation for different mode shapes and to obtain their natural frequencies. Meanwhile, DMD has good capabilities for frequency isolation and mode shape estimation. However, it has issues when sorting the modes obtained and correlating between the full structure and the substructure.

For future work, different directions can be pursued. One of the issues with the current simulation is that many of the points extracted possess similar mode shape responses at different frequencies. A better DOF selection for the BARC could give orthogonal mode shapes, which can facilitate the correlation between the reconstructed models obtained from DMD and PCA for the full and substructure. In addition, currently, the Koopman operator estimation for the exact DMD works only for full-rank approximation, leading to a high computational cost for cases where the number of DOFs extracted is high. More investigation into the algorithm and how to more effectively employ it to substructure problems will be conducted in the future.

Acknowledgments This work is supported by the Department of Energy Kansas City National Security Campus Managed by Honeywell under contract # N000510678.

References

1. D. De Klerk, D. J. Rixen, and S. N. Voormeeren, "General framework for dynamic substructuring: history, review and classification of techniques," AIAA journal, vol. 46, no. 5, pp. 1169-1181, 2008.
2. M. S. Allen, D. Rixen, M. Van der Seijs, P. Tiso, T. Abrahamsson, and R. L. Mayes, Substructuring in engineering dynamics. Springer, 2020.
3. F. M. Gruber and D. J. Rixen, "Evaluation of substructure reduction techniques with fixed and free interfaces," Strojniški vestnik-Journal of Mechanical Engineering, vol. 62, no. 7-8, pp. 452-462, 2016.
4. E. Lindberg, N.-E. Hörlin, and P. Göransson, "Component mode synthesis using undeformed interface coupling modes to connect soft and stiff substructures," Shock and vibration, vol. 20, no. 1, pp. 157-170, 2013.
5. R. J. Kuether, M. S. Allen, and J. J. Hollkamp, "Modal substructuring of geometrically nonlinear finite element models with interface reduction," AIAA Journal, vol. 55, no. 5, pp. 1695-1706, 2017.
6. D. E. Soine, R. J. Jones, J. M. Harvie, T. J. Skousen, and T. F. Schoenherr, "Designing hardware for the boundary condition round robin challenge," in Topics in Modal Analysis & Testing, Volume 9: Proceedings of the 36th IMAC, A Conference and Exposition on Structural Dynamics 2018, 2018: Springer, pp. 119-126.
7. T. F. Schoenherr, "Derivation of six degree of freedom shaker inputs using sub-structuring techniques," in Topics in Modal Analysis & Testing, Volume 9: Proceedings of the 36th IMAC, A Conference and Exposition on Structural Dynamics 2018, 2018: Springer, pp. 5-14.
8. R. Schultz, T. Schoenherr, and B. Owens, "A proposed standard random vibration environment for BARC and the boundary condition challenge," in Sensors and Instrumentation, Aircraft/Aerospace, Energy Harvesting & Dynamic Environments Testing, Volume 7: Proceedings of the 39th IMAC, A Conference and Exposition on Structural Dynamics 2021, 2021: Springer, pp. 77-84.
9. S. Chirinos, A. Pawar, H. Tholen, S. Ouellette, and T. Roberts, "Parametric Simulations of the BARC Model in SDOF and MIMO Configurations for Estimating Service Environment Severity," in Sensors and Instrumentation, Aircraft/Aerospace and Dynamic Environments Testing, Volume 7: Proceedings of the 40th IMAC, A Conference and Exposition on Structural Dynamics 2022, 2022: Springer, pp. 19-40.
10. J. M. Harvie and M. van der Seijs, "Application of transfer path analysis techniques to the boundary condition challenge problem," in Sensors and Instrumentation, Aircraft/Aerospace, Energy Harvesting & Dynamic Environments Testing, Volume 7: Proceedings of the 37th IMAC, A Conference and Exposition on Structural Dynamics 2019, 2019: Springer, pp. 157-166.
11. U. Musella et al., "Combining test and simulation to tackle the challenges derived from boundary conditions mismatches in environmental testing," in Sensors and Instrumentation, Aircraft/Aerospace, Energy Harvesting & Dynamic Environments Testing, Volume 7: Proceedings of the 37th IMAC, A Conference and Exposition on Structural Dynamics 2019, 2019: Springer, pp. 259-269.
12. P. J. Schmid, "Data-driven and operator-based tools for the analysis of turbulent flows," in Advanced Approaches in Turbulence: Elsevier, 2021, pp. 243-305.
13. H.-W. Ma, Y.-Z. Lin, and Z.-H. Nie, "Physical interpretation of principal component analysis for structural dynamics through string vibration," International Journal of Structural Stability and Dynamics, vol. 19, no. 09, p. 1950109, 2019.
14. E. Aoki, C. T. do Cabo, Z. Mao, Y. Ding, and S. Ozharar, "Vibration-Based Status Identification of Power Transmission Poles," IFAC-PapersOnLine, vol. 55, no. 27, pp. 214-217, 2022.
15. P. J. Schmid, "Dynamic mode decomposition of numerical and experimental data," Journal of fluid mechanics, vol. 656, pp. 5-28, 2010.
16. J. H. Tu, "Dynamic mode decomposition: Theory and applications," Princeton University, 2013.
17. J. N. Kutz, S. L. Brunton, B. W. Brunton, and J. L. Proctor, Dynamic mode decomposition: data-driven modeling of complex systems. SIAM, 2016.
18. N. A. Valente, C. T. do Cabo, Z. Mao, and C. Niezrecki, "Dynamic Mode Decomposition for Resonant Frequency Identification of Oscillating Structures," in Society for Experimental Mechanics Annual Conference and Exposition, 2023: Springer, pp. 155-162.
19. S. L. Brunton, "Notes on Koopman operator theory," Universität von Washington, Department of Mechanical Engineering, Zugriff, vol. 30, 2019.
20. T. Askham and J. N. Kutz, "Variable projection methods for an optimized dynamic mode decomposition," SIAM Journal on Applied Dynamical Systems, vol. 17, no. 1, pp. 380-416, 2018.